A heat engine made of quantum dot molecules with high figure of merits

Chih-Chieh Chen,[1] David M T Kuo[2] and Yia-Chung Chang[1,3,4]
[1]Department of Physics, University of Illinois at Urbana-Champaign, Urbana, Illinois 6180, USA
[2]Department of Electrical Engineering and Department of Physics,
National Central University, Chungli, 320 Taiwan
[3]Research Center for Applied Sciences, Academic Sinica, Taipei, 11529 Taiwan and
[4] Department of Physics, National Cheng Kung University, Tainan, 701 Taiwan
(Dated: January 6, 2016)

The transport of electrons through serially coupled quantum dot molecules (SCQDM) is investigated theoretically for application as an energy harvesting engine (EHE), which converts thermal heat to electrical power. We demonstrate that the charge current driven by a temperature bias shows bipolar oscillatory behavior with respect to gate voltage due to the unbalance between electrons and holes, which is different from the charge current driven by an applied bias. In addition, we reveal a Lenz's law between the charge current and the thermal induced voltage. The efficiency of EHE is higher for SCQDM in the orbital depletion situation rather than the orbital filling situation, owing to the many-body effect. The EHE efficiency is enhanced with increasing temperature bias, but suppressed as the electron hopping strength reduces. The fluctuation of QD energy levels at different sites also leads to a reduction of EHE efficiency. Finally, we demonstrate direction-dependent charge currents driven by the temperature bias for application as a novel charge diode.

I. INTRODUCTION

Energy harvesting of heat dissipated from electronic circuits and other heat sources is one of the most important energy issues.[1] The realization of such type of energy harvesting typically relies on the search of thermoelectric (TE) materials with high figure of merits (ZT).[2] Impressive ZT values for quantum-dot superlattices (QDSL) systems have been demonstrated experimentally.[3] The enhancement of ZT mainly arises from the reduction of phonon thermal conductivity in QDSL, which is due to the increased rate of phonon scattering from the interface of quantum dots (QDs).[1,2] If the ZT value can reach 3, the solid state cooler will have the potential to replace conventional compressor-based air conditioners owing to its long life time, low noise and low air pollution. Besides the search of TE devices with large ZT value, the optimizing of nonlinear thermoelectric behavior under high temperature bias is crucial for the design of the next-generation energy harvesting engine (EHE).[1,2]

Recently, a grate deal of efforts was devoted to the studies of the nonlinear response of thermoelectric devices under high temperature bias. The nonlinear phonon flow of nanostructures with respect to large temperature bias were investigated experimentally[4] and theoretically.[5-8] The phonon thermal rectification behavior of silicon nanowire (which has a very low efficiency) was reported experimentally.[4] More recently, the highly efficient electron thermal diode was reported in a superconductor junction system.[9] However, such a thermal rectification behavior only exists at very low temperatures. Unlike heat rectifiers which are used to control the direction of heat flow [4-9], the design of an EHE driven by a large temperature bias needs to optimize the efficiency in the energy transfer from the waste heat[1,2]. To design a nanoscale EHE, which can be integrated with semiconductor electronic circuits, it is important not only to collect the waste heat but also to improve the performance of electronic circuits.

So far, experimental studies of EHE made of semiconductor QD molecules (QDMs) have not been reported, mainly due to technical difficulties and the lack of theoretical designs. Therefore, it is desirable to have theoretical studies which can provide useful guidelines for the advancement of nanoscale TE technology. Most theoretical studies of TE properties are limited in the linear response regime.[10-13] The many-body effect of QDMs also presents a big challenge to the development of theoretical studies for TE properties. In this article, we study the nonlinear behavior of EHE made of serially coupled triple QDs (SCTQDs) based on a previously developed numerically method,[12,13] which can suitably address the many body effect in the Coulomb blockade regime. In addition, we investigate an engine with direction-dependent electrical output driven by a temperature-bias for application as a novel nonlinear TE devices.

II. FORMALISM

The inset of Fig. 1(a) shows the QD molecule (QDM) connected to two metallic electrodes, one is in thermal contact with the heat source at temperature T_H (hot side) and the other with the heat sink kept at temperature T_C (cold side). The heat flows from the hot side through the QDM into the cold side. To reveal the charge and heat currents driven by the temperature bias, we consider the following Hamiltonian $H = H_0 + H_{QD}$ for a SCTQDs:

$$H_0 = \sum_{k,\sigma} \epsilon_k a^{\dagger}_{k,\sigma} a_{k,\sigma} + \sum_{k,\sigma} \epsilon_k b^{\dagger}_{k,\sigma} b_{k,\sigma} + \sum_{k,\sigma} V_{k,L} d^{\dagger}_{L,\sigma} a_{k,\sigma} + \sum_{k,\sigma} V_{k,R} d^{\dagger}_{R,\sigma} b_{k,\sigma} + c.c \quad (1)$$

where the first two terms describe the free electron gas of left and right electrodes (hot and cold sides). $a^{\dagger}_{k,\sigma}$ ($b^{\dagger}_{k,\sigma}$) creates an electron of momentum k and spin σ with energy ϵ_k in the left (right) electrode. $V_{k,\ell}$ ($\ell = L, R$) describes the coupling between the electrodes and the left (right) QD. $d^{\dagger}_{\ell,\sigma}$ ($d_{\ell,\sigma}$) creates (destroys) an electron in the ℓ-th dot.

$$H_{QD} = \sum_{\ell,\sigma} E_\ell n_{\ell,\sigma} + \sum_{\ell} U_\ell n_{\ell,\sigma} n_{\ell,\bar{\sigma}} + \frac{1}{2} \sum_{\ell,j,\sigma,\sigma'} U_{\ell,j} n_{\ell,\sigma} n_{j,\sigma'} + \sum_{\ell,j,\sigma} t_{\ell,j} d^{\dagger}_{\ell,\sigma} d_{j,\sigma}, \quad (2)$$

where E_ℓ is the spin-independent QD energy level, and $n_{\ell,\sigma} = d^{\dagger}_{\ell,\sigma} d_{\ell,\sigma}$. Notations U_ℓ and $U_{\ell,j}$ describe the intradot and interdot Coulomb interactions, respectively. $t_{\ell,j}$ describes the electron interdot hopping. Noting that the interdot Coulomb interactions as well as intradot Coulomb interactions play a significant role on the charge transport in semiconductor QD arrays or molecular chains.[10-13] Because we are interested in the case that the thermal energy is much smaller than intradot Coulomb interactions, we consider QDs with only one energy level per dot.

Using the Keldysh-Green's function technique,[14,15] the charge and heat currents from reservoir α to the QDM junction are calculated according to the Meir-Wingreen formula

$$J_\alpha = \frac{ie}{h} \sum_{j\sigma} \int d\epsilon \Gamma^{\alpha}_{j}(\epsilon) [G^{<}_{j\sigma}(\epsilon) + f_\alpha(\epsilon)(G^{r}_{j\sigma}(\epsilon) - G^{a}_{j\sigma}(\epsilon))] \quad (3)$$

$$Q_\alpha = \frac{i}{h} \sum_{j\sigma} \int d\epsilon (\epsilon - \mu_\alpha) \Gamma^{\alpha}_{j}(\epsilon) [G^{<}_{j\sigma}(\epsilon) f_\alpha(\epsilon) (G^{r}_{j\sigma}(\epsilon) - G^{a}_{j\sigma}(\epsilon))], \quad (4)$$

Notation $\Gamma^{\alpha}_{\ell} = \sum_k |V_{k,L(R),\ell}|^2 \delta(\epsilon - \epsilon_k)$ is the tunneling rate between the left (right) reservoir and the left (right) QD of QDM. $f_\alpha(\epsilon) = 1/\{\exp[(\epsilon - \mu_\alpha)/k_B T_\alpha] + 1\}$ denotes the Fermi distribution function for the α-th electrode, where μ_α and T_α are the chemical potential and the temperature of the α electrode. $\mu_L - \mu_R = e\Delta V$ and $T_L - T_R = \Delta T$. e, h, and k_B denote the electron charge, the Planck's constant, and the Boltzmann constant, respectively. $G^{<}_{j\sigma}(\epsilon)$, $G^{r}_{j\sigma}(\epsilon)$, and $G^{a}_{j\sigma}(\epsilon)$ are the frequency domain representations of the one-particle lesser, retarded, and advanced Green's functions $G^{<}_{j\sigma}(t,t') = i\langle d^{\dagger}_{j,\sigma}(t') d_{j,\sigma}(t)\rangle$, $G^{r}_{j\sigma}(t,t') = -i\theta(t-t')\langle\{d_{j,\sigma}(t), d^{\dagger}_{j,\sigma}(t')\}\rangle$, and $G^{a}_{j\sigma}(t,t') = i\theta(t'-t)\langle\{d_{j,\sigma}(t), d^{\dagger}_{j,\sigma}(t')\}\rangle$, respectively. These one-particle Green's functions are related recursively to other Green's functions and correlation functions via a hierarchy of equations of motion (EOM). To clarify the nonlinear thermal behavior of EHE in the Coulomb blockade regime, we numerically solve Eqs. (3) and (4) by considering all correlation functions and Green's functions.[12,13] To design an EHE driven by an applied temperature-bias, the thermal induced voltage ($eV_{th} = \mu_L - \mu_R$) across the external load with conductance G_{ext} needs to be calculated for a given temperature bias ΔT. To obtain eV_{th}, we have to solve self-consistently all correlation functions appearing in Eq. (3) subject to the condition $G_{ext} V_{th} + J = 0$, where $J = (J_L + J_R)/2$ is the net charge current. The heat current satisfies the condition $Q_L + Q_R = -J * V_{th}$, which denotes the work done by the EHE per unit time. The efficiency of EHE is thus given by

$$\eta = |J * V_{th}|/Q_L. \quad (5)$$

To reveal the importance of many-body effect, which is fully accounted for in the numerical method,[12,13] we rewrite the net charge and heat currents as[16]

$$J = \frac{e}{h} \int d\epsilon \mathcal{T}_{LR}(\epsilon)[f_L(\epsilon) - f_R(\epsilon)], \quad (6)$$

and

$$Q_{L/R} = \pm\frac{1}{h} \int d\epsilon \, (\epsilon - \mu_{L(R)}) \mathcal{T}_{LR}(\epsilon)[f_L(\epsilon) - f_R(\epsilon)]. \quad (7)$$

Notation $\mathcal{T}_{LR}(\epsilon)$ is the transmission coefficient for electron transport through the QDMs. Because there are four possible states for each QD level (empty, one spin-up electron, one spin-down electron, and two electrons), $\mathcal{T}_{LR}(\epsilon)$ contains $4^3 = 64$ configurations for the SCTQD. The analytical expression of $\mathcal{T}_{LR}(\epsilon)$ can be found in [16],in which only one-particle occupation numbers and two-particle on-site correlation functions used in the Green's functions are considered. We shall demonstrate that the method of [16] is a good approximation for QDMs in the low-filling regime.

III. RESULTS AND DISCUSSION

Figure 1(a) shows the total occupation number ($N_t = \sum_\sigma (\langle n_{L\sigma}\rangle + \langle n_{C\sigma}\rangle + \langle n_{R\sigma}\rangle$) of SCTQD without thermal bias ($k_B \Delta T = 0$) as a function of the applied gate voltage V_g (which can tune the QD energy level according to $E_\ell = E_F + 30\Gamma_0 - eV_g$) for three different temperatures ($k_B T_C = 1, 3, 5\Gamma_0$). The electric bias is set at $e\Delta V = -1\Gamma_0$. The staircase behavior of N_t is due to the charging effect arising from electron intradot and interdot Coulomb interactions. The plateaus of N_t correspond to numbers of integer charges in the SCTQD as electrons fill the QD levels in the Coulomb blockade regime. The average occupancies in the center dot ($\langle n_{C\sigma}\rangle = N_{C,\sigma}$) and outer dots ($\langle n_{L\sigma}\rangle(N_{L,\sigma}) = \langle n_{R\sigma}\rangle(N_{R,\sigma})$) are also plotted in Fig. 1(a) as dash-double-dots and dash-dotted curves, respectively. Because of symmetry, the average occupancies in two outer dots remain the same as V_g varies, which leads to a jump of 2 for N_t for the first two steps. The corresponding tunneling currents $J_{\Delta V}$ are plotted in Fig. 1(b). The negative sign of $J_{\Delta V}$ indicates that charge carriers are flowing from the right electrode to the left electrode. The tunneling currents are appreciable only in the regions where N_t jumps a step, but become blocked when N_t is flat as a function of eV_g. In the absence of electron Coulomb interactions, there are three resonant channels of $\epsilon = E_0 - \sqrt{2}t_c$, $\epsilon = E_0$ and $\epsilon = E_0 + \sqrt{2}t_c$. When $\epsilon_1 = E_0 - \sqrt{2}t_c = E_F + 30\Gamma_0 - \sqrt{2}t_c$ is aligned with the E_F of electrodes, we reach the maximum of the ϵ_1 peak. Once $E_L = E_R$ are well below E_F, the central QD is depleted (see the curve labeled by $\langle n_{C\sigma}\rangle$). Meanwhile,the outer QDs are filled with one electron for each QD ($\langle n_{L\sigma}\rangle + \langle n_{R\sigma}\rangle = 1$). The situation remains unchanged until the energy level of $\epsilon_2 \approx E_C + U_{LC} + U_{CR}$ is aligned with E_F, one electron is filled into the central QD. The peak of ϵ_2 describes the three-electron process. For example, one electron with spin up (down) of the left electrode tunnels into the left QD with spin down (up) via the energy level of $E_C + U_{LC} + U_{CR}$ and transfer to the right QD with spin down (up). Such a three-electron process is blockaded with increasing the gate voltage. When $E_L + U_L$ and $E_R + U_R$ are below E_F, the increasing two electron occupation probability weight of outer QDs ($\sum_\sigma(N_{L,\sigma} + N_{R,\sigma}) = 4$) suppresses the probability of three-electron process. Although one electron is injected into the central QD when $E_C + 2U_{LC} + 2U_{CR}$ is aligned with E_F, the transport probability of this five electrons of SCTQD molecule is extremely small due to $(E_C + 2U_{LC} + 2U_{CR})$not line up with $E_L + U_L + U_{LC}$ and $E_R + U_R + U_{CR}$. Note that these plateaus are washed out with increasing temperature. The Hartree-Fock approximation method widely used for molecular junctions can not reveal the charge transport through molecules in the Coulomb blockade regime.[10,11] The maximum currents prefers the orbital-depletion regime of SCTQDs molecule. J_{max} is suppressed with increasing temperature (T_C). Fig. 1(c) shows the charge current driven by a temperature bias for various values of k_BT_C with $\Delta V = 0$. Unlike $J_{\Delta V}$, $J_{\Delta T}$ shows the bipolar Coulomb oscillatory behavior with respect to eV_g. Positive (negative) sign indicates that $J_{\Delta T}$ is from the left (right) electrode to the right (left) electrode. When QD energy levels are above E_F, electrons of the left (hot) electrode diffuse into the right (cold) electrode by a temperature bias. On the other hand, electrons of the cold electrode can diffuse into the hot electrode when QD energy levels are below E_F. In general, we introduce "the hole picture", which is defined as the states below E_F without electron occupation, to illustrate the behavior of negative $J_{\Delta T}$. When electron hole balances, $J_{\Delta T}$ vanishes. The sign change of $J_{\Delta T}$ as V_g varies indicates a bipolar effect. Such a behavior is very different from the charge current driven by an applied bias $e\Delta V$. It is worth noting that the maximum $J_{\Delta T}$ is suppressed with increasing T_C. Recently, the bipolar behavior of $J_{\Delta T}$ was experimentally reported in a single metallic QD junction system.[17]

In the operation of EHE, a temperature bias ΔT should induce a thermal voltage V_{th} ($eV_{th} = \mu_L - \mu_R$) which depends on the load conductance G_{ext}. Fig. 2(a) shows the charge current (J) driven by a temperature bias, $k_B\Delta T = 1\Gamma_0$ at various values of k_BT_C. We see that the behavior of charge current shown in Fig. 2(a) is similar to that of Fig. 1(c) with zero load resistance (i.e $1/G_{ext} = 0$), which display a bipolar Coulomb oscillatory behavior. Fig. 2(b) shows the thermal voltage V_{th} induced by ΔT. This thermal voltage has two kinds of characteristics. The sign of eV_{th} is opposite to that of J. Meanwhile, the magnitude of V_{th} is in proportion to J. This counter active behavior of V_{th} and J is related the Lenz's law in TE effect. Fig. 2(c) shows the the EHE efficiency, η for various values of T_C. It is seen that the peak values of η is suppressed as T_C/T_H increases and η reduces to zero as T_C/T_H approaches 1 (i.e $\Delta T = 0$). Such a behavior is similar to a Carnot engine or an ideal TE device (with ZT approaching infinity), for which the efficiency is given by $\eta_C = (1 - T_C/T_H)$.[1,2] From the results of Fig. 2, we see that the highest efficiency of EHE occurs near the transition where N_t goes from 0 to 1 (with $eV_g \approx 25\Gamma_0$), which is in the low-filling regime. When QD energy levels are below E_F, not only the charge current but also the EHE efficiency is suppressed owing to the strong electron correlation. The EHE of a single QD with one energy level was theoretically discussed without considering V_{th} and electron Coulomb interactions in references [18-19]. The approach considered in references [18-20] is similar to the case discussed in Fig. 1, where ΔT and ΔV are unrelated. Based on the approach of references of [18-20], the Lenz's law will not apply.

To reveal the importance of electron correlation arising from many body effect, the physical quantities of Fig. 2 are recalculated by Eqs. (6) and (7), where for the transmission factor, $\mathcal{T}_{LR}(\epsilon)$ we include only the one-particle occupation number for each QD and intradot two-particle correlation functions[16]. The resulting curves are shown in Fig. 3, which have one-to-one correspondence to those of Fig. 2. For the low-filling situation (with $eV_g < 30\Gamma_0$), the results agree very well with the full-calculation results shown in Fig. 2. On the other hand, there are appreciable differences between the two results as N_t exceeds 1 (with $eV_g > 30\Gamma_0$), although their behaviors are qualitatively the same for eV_g up $100\Gamma_0$. This implies that a simplified model without considering interdot correlation functions is sufficient to model the main characteristics of the EHE made of SCTQDs in the low-filling regime ($N_t \leq 1$).

It is difficult to analyze the physical mechanisms for the charge current given in Eq. (3) in the nonlinear regime. In stead, we can analyze Eq. (6) in the linear response regime, where we have $J = J_{\Delta V_{th}} + J_{\Delta T} = \mathcal{L}_0\Delta V_{th} +$

$\mathcal{L}_1\Delta T$. The charge current now has two driving forces, namely ΔV_{th} and ΔT. The thermoelectric coefficient $\mathcal{L}_n$ can be expressed as

$$\mathcal{L}_n = \frac{2e^2}{h}\int d\epsilon \mathcal{T}_{LR}(\epsilon)(\frac{(\epsilon - E_F)}{eT})^n \frac{\partial f(\epsilon)}{\partial E_F}, \quad (8)$$

where $f(\epsilon) = 1/(exp^{(\epsilon - E_F)/k_BT} + 1)$ is the equilibrium Fermi distribution function and T denotes the equilibrium temperature of electrodes. $J_{\Delta V_{th}}$ and $J_{\Delta T}$ for the first resonant channel in the weak-tunneling limit, $\Gamma/k_BT \ll 1$ can be expressed as

$$J_{\Delta V_{th}} = \frac{2e^2}{h}\frac{\pi\Gamma P_1}{k_BT}\frac{4t_{LC}^2t_{CR}^2}{(t_{LC}^2+t_{CR}^2+\Gamma^2)^2}\frac{\Delta V_{th}}{cosh^2\frac{E_0-E_F}{2k_BT}}. \quad (9)$$

$$J_{\Delta T} = \frac{2e}{h}\frac{\pi\Gamma P_1}{k_BT^2}\frac{4t_{LC}^2t_{CR}^2(E_0-E_F)}{(t_{LC}^2+t_{CR}^2+\Gamma^2)^2}\frac{\Delta T}{cosh^2\frac{E_0-E_F}{2k_BT}}, \quad (10)$$

where $P_1 = (1 - N_{L,\bar{\sigma}})(1 - N_{C,\sigma} - N_{C,\bar{\sigma}} + c_C)(1 - N_{R,\sigma} - N_{R,\bar{\sigma}} + c_R)$ denotes the probability weight of SCTQDs with an empty state, which is determined by the single particle occupation number (N_ℓ) and intradot two particle correlation functions (c_ℓ).[16] From Eqs. (9) and (10), we see that the maximum $J_{\Delta V_{th}}$ and $J_{\Delta T}$ occur at $t_{LC} = t_{CR}$. Thus, inhomogenous electron hopping strength will reduce J. When we consider an open circuit ($G_{ext} = 0$), the linear Seebeck coefficient ($S = \Delta V_{th}/\Delta T = -(E_0 - E_F)/(eT)$) provides the behavior of ΔV_{th}, which is irrelevant with $t_{\ell,j}$, U_ℓ, $U_{\ell,j}$ and Γ.[16] The bipolar behavior of Figs. 1(c) and 2(a) can be explained by Eq. (10).

So far, we have fixed $G_{ext} = 0.2G_0$, where $G_0 = 2e^2/h$ is the quantum conductance. The case of $G_{ext} = 0$ was studied in our previous studies for the design of electronic thermal rectifiers.[7,8] In the inset of Fig. 3, we plot $\eta = |J \times V_{th}|/(Q_L + Q_{ph})$ versus V_g for four different values of G_{ext} at $k_BT_c = 1\Gamma_0$, $k_B\Delta T = 1\Gamma_0$ and $t_C = 1\Gamma_0$. Note that the calculations of results shown in the inset include the effect of phonon heat flow given by $Q_{ph} = \kappa_{ph,0}F_s\Delta T$, where $\kappa_{ph,0} = \frac{\pi^2k_B^2\bar{T}}{3h}$ is the universal phonon thermal conductance arising from acoustic phonon confinement in a nanowire. $F_s = 0.1$ when one considers the phonon scattering from QDs embedded in a nanowire.[16] $\bar{T} = (T_C + T_H)/2$. The maximum efficiency is obtained at $G_{ext} = 0.05G_0$. Meanwhile, the maximum η for $G_{ext} = 0.2G_0$ (blue line) is around 0.08 including the effect of Q_{ph}, which is much smaller than the value obtained with $Q_{ph} = 0$ as shown by the black solid line of Fig. 3.

To understand the effect of G_{ext} shown in the inset, we can also compare with the η derived by classical approach considered in references[1,2] and obtain

$$\eta = (1 - \frac{T_C}{T_H})\frac{m}{m + (1+m)^2/(ZT_H) + \bar{T}/T_H}, \quad (11)$$

where $m = G_e/G_{ext}$, and $Z = \frac{S^2G_e}{\kappa}$. G_e, $S = V_{th}/\Delta T$, and κ are the internal electrical conductance, Seebeck coefficient and thermal conductance of the TE device. By taking $d\eta/dm|_{m_o} = 0$, we obtain $m_o = G_e/G^o_{ext} = \sqrt{1 + Z\bar{T}}$, which gives the maximum value of η. Because $G^o_{ext} = G_e/\sqrt{1 + Z\bar{T}}$, η_{max} will occur at vanishingly small G_{ext} if $Z\bar{T}$ becomes very large, and the limit of Carnot engine with $\eta_{max} = (1 - T_c/T_H)$ is reached). When $Z\bar{T} = 2$, $G^0_{ext} = G_e/\sqrt{3} \approx 0.047G_0$ for $G_e = 0.08G_0$. In the Coulomb blockaded regime, G_e is much smaller than G_0 for k_BT/Γ larger than 1.[See Eq. (9)] The behavior of results shown in the inset of Fig. 3 can be explained by Eq. (11). Previously, we demonstrated that the ZT of SCQDM can be larger than 2, including the effect of phonon heat flow.[16]. This implies that QDMs have promising potential for realizing high-efficiency EHEs.

To further examine the behavior of the EHE efficiency, we plot in Fig. 4 J, Q_L and η as functions of V_g for various values of $k_B\Delta T$ with T_C fixed at $1\Gamma_0$. We see that the peak values of J, Q_L and η all increases with ΔT. The results of Fig. 4 indicate that a high efficiency engine with large electrical outputs needs to maintain a high temperature bias, which in general only exists in systems with high thermal resistivity (phonon glass). Serially coupled QDs can enhance the phonon scattering and thus reduce thermal conductivity. Therefore, a long chain of QD molecules is more suitable than a short chain for implementing EHE with high efficiency. From the results of Figs. (2) and (4), designers can focus on the EHE operated at the low-filling regime instead of high-filling situations. In the low-filling regime, one can usually ignore the interdot Coulomb interactions, whereas the intradot Coulomb interactions still play an important role for the electron transport in the Coulomb blockade regime.[13] Because the effect of Q_{ph} is important as shown in the inset in Fig. 3, we also show the result including the Q_{ph} effect by triangle marks (with $k_B\Delta T = 3\Gamma_0$), which is to be compared with the dotted line of Fig. 4(c), Obviously, η_{max} is suppressed when Q_{ph} is included.

We have adopted $t_c = 1\Gamma_0$ in Figs (1)-(4). t_c should depend on the separation between QDs. To clarify the effect of t_c on the efficiency of EHE, we plot in Fig. 5 the charge current (J), thermal voltage (V_{th}), and efficiency (η) as functions of V_g for various values of t_c. From the expressions of Eq. (10), the charge current is proportional to t_c^4 in the weak tunneling limit, $t_c/\Gamma \ll 1$. When $t_c \geq \Gamma$, the maximum of J no longer increases with increasing t_c. The behavior of J with respect to t_c is consistent with the expression of Eq. (10), although it is solely valid in the linear response regime. Next, we see that V_{th} still follows the Lenz's law with respect to J. The results of Fig. 5(c) show that the maximum η occurs at $t_c = 1\Gamma$. Had we not considered the self-consistent solution of V_{th}, the maximum η would have occurred at $t_c \to 0$.[20] Obviously, the self-consistent treatment of V_{th} is essential for getting physically meaningful results. Recently, the thermal voltage yielded by temperature bias for the metallic coupled QD was experimentally reported at very low temperatures [21]. Due to metallic coupled QD, the temperature bias is still in linear response regime.[21] Meanwhile, we note that J always vanishes at $E_0 - E_F = 0$. This is well illustrated by Eq. (10). Due to Lenz's law, V_{th} also vanishes at $E_0 = E_F$ (see Fig. 5(b)).

When there is size/shape variation in serially coupled QDs, the energy level fluctuation (ELF) of QDs will cause a significant effect on the ZT values.[16] Therefore, it is desirable to examine the ELF effect on the charge current and EHE efficiency of SCTQD. The effects of ELF at different sites of SCTQD are shown in Fig. 6. It can be seen from Fig. 6 that the charge current reduces quickly as the difference in QD energy levels becomes larger than the coupling, t_c. We found that the effect of ELF for the central QD is smaller than that for outer QD. Meanwhile, the temperature effect shown in Fig. 6(a) is very different from the results shown in Figs. 1 and 2, where the peak width increases significantly with increasing temperature T_C. The results of Fig. 6(a) imply that the width of peaks depends on parameters such as tunneling rates and electron hopping strengths, but not on T_C. Such behavior can be understood by the long distance coherent tunneling effect (LDCT).[12,13,22] When $E_C \neq E_L = E_R$, it will introduce an effect hopping strength $t_{eff} = -t_{LC}t_{CR}/(E_C - E_R)$ between the outer QDs. The behavior of curves shown in Fig. 6(b) is called the nonthermal broadening effect as reported for the DQD case, where the peak width depends only on the tunneling rate.[23] Such characteristics can be used to determine the coupling strength between QDs and electrodes. They are also useful for applications in low temperature filters.[23]

Although the EHE efficiency is suppressed by ELF in SCTQDs, such phenomenon can be used to design an engine with direction-dependent electrical output. In Figs. 7(a) and 7(b), the charge current (J) and thermal voltage (V_{th}) are calculated for an SCTQD with the staircase energy levels of $E_L = E_R + 2\Delta$, $E_C = E_R + \Delta$ and $E_R = E_F + 10\Gamma_0$, where Δ is the QD energy level difference. In our calculations, the change of outer QD energy levels arising from V_{th} has been included. Namely, the outer QD levels become $\epsilon_{L(R)} = E_{L(R)} \pm D_\eta V_{th}$. It's worth noting that the tunable factor $D_\eta = 0.3$ is mainly determined by the QD separation.[22] For $\Delta T > 0$, T_H is on the left electrode. For $\Delta T < 0$, the two sides are swapped. (See insets of Fig. 7(a)) The forward (backward) currents ($J_{F(B)}$) are positive (negative), while V_{th} has opposite sign with respect to J. Thus, the Lenz's law between J and V_{th} is maintained. For both forward and backward currents, the charge currents have a nonlinear dependence on ΔT. With increasing Δ, the charge currents (or electrical powers) are suppressed in the wide temperature bias regime. For $\Delta = 0$ (solid black curve), the charge currents shows no directionality, while for $\Delta = 2\Gamma_0$ the direction-dependent charge current becomes apparent. This directionality of charge current can be qualitatively explained as follows. When $\Delta T > 0$, ϵ_L and ϵ_R become aligned with E_C as eV_{th} changes to around $-2\Gamma_0$, while for $\Delta T < 0$, ϵ_L and ϵ_R are tuned further away from E_C. Therefore, QD energy level shift due to the thermal voltage induced by the temperature-bias can play a remarkable role for the current rectification effect in SCTQD with staircase-like energy levels.

Let's define the charge current rectification efficiency as $\eta_R = (J_F - |J_B|)/(J_F + |J_B|)$, which is irrelevant to heat flows. The calculated η_R as a function of temperature bias under various conditions is shown in Fig. 8. Figure 8(a) shows η_R for various values of Δ with $t_C = 3\Gamma_0$. We see that the highest rectification occurs when $\Delta = 2\Gamma_0$ with η_R approaching 0.2 at the high ΔT limit. The rectification efficiency actually becomes poorer if Δ is too large. Unlike the case with $\Delta = 2\Gamma_0$, η_R decreases with increasing ΔT for $\Delta = 4$ and $6\Gamma_0$. To reveal the electron correlation effects, we also calculate η_R with the simplified procedure as described in Ref.[16] and plot the corresponding curves with triangle marks in Fig. 8(a). It is found that the rectification efficiency over estimated in the simplified model. Figure 8(b) shows η_R at $\Delta = 2\Gamma_0$ for different electron hopping strengths ($t_C = 0.5, 1$, and $2\Gamma_0$). η_R is found to be largest for $t_c = 2\Gamma_0$ (dotted line), which is also larger than that for $t_c = 3\Gamma_0$ as shown in Fig. 8(a). Thus, the charge current rectification efficiency is not a monotonic function of t_c, which is similar to that of Fig. 5(c). In Fig. 8(c), we consider the effect of varying the temperature of the cold side, T_C. The results indicate that the maximum η_R reduces with increasing T_C.

Recently, the nonlinear thermoelectric effects of nanostructures for developing new applications have been reviewed.[24] For phonon rectifiers, it is very difficult to realize "phonontronics" due to large leakage of phonon flow arising from acoustic phonons, which lack suitable phonon confinement.[4-6,24] The heat rectification phenomena of electrons can only exist in the very low temperature regime, because it is seriously suppressed by phonon flows.[7-9,25] On the other hand, the charge current rectification shown in Fig. 7 will be unaffected by the phonon flow. Therefore an EHE made of serially coupled QDs with direction-dependent electrical current may prove useful in the advancement of nonlinear thermoelectric devices.[26]

IV. SUMMARY

The charge and heat transport through SCTQD driven by a temperature-bias is theoretically studied for the application of EHE which convert the thermal energies into electrical power. This study clarifies the efficiency of EHE by considering the self-consistent solution of charge current with the condition of $G_{ext}\ V_{th} + J = 0$. We have demonstrated that EHE prefers the SCTQDs with energy levels above the Fermi energy of electrodes (orbital depletion situation). The maximum efficiency of EHE is not necessary to occur at the maximum electrical output. We found that J is degraded by the position-dependent QD ELF, which may arise from QD size fluctuation or energy level shift resulting from V_{th}. η_{max} of EHE is seriously suppressed in the presence of phonon thermal conductance. QDMs have promising potential for realizing high-efficy EHEs due to their low phonon thermal conductance. The direction-dependent charge current is illustrated by the SCTQDs with staircase energy levels. The thermal voltage yielded by a temperature bias plays a remarkable role to design a engine with directionality driven by a temperature bias. This study can be extended to the reversed process of Seebeck effect (nonlinear behavior of Peltier effect) for the application of nanoscale coolers.

Acknowledgments

This work was supported by the National Science Council of the Republic of China under Contract Nos. MOST 103-2112-M-008-009-MY3 and MOST 104-2112-M-001-009-MY2.

E-mail address: mtkuo@ee.ncu.edu.tw
E-mail address: yiachang@gate.sinica.edu.tw

[1] A. J. Minnich,M. S. Dresselhau, Z. F. Ren, and G. Chen, Energy Environ, Sci. **2**, 466 (2009).
[2] M. Zebarjadi, K. Esfarjania, M.S. Dresselhaus, Z.F. Ren and G. Chen, Energy Environ Sci **5**, 5147 (2012).
[3] T. C. Harman, P. J. Taylor, M. P. Walsh, B. E. LaForge, Science **297**, 2229 (2002).
[4] C. W. Chang, D. Okawa, A. Majumdar, and Zettl A, Science **314**, 1121 (2006).
[5] B. W. Li, L. Wang and G. Casati, Phys. Rev. Lett, Phys. Rev. Lett. **93**, 184301 (2004).
[6] B. Hu, L. Yang, and Y. Zhang, Phys. Rev. Lett. **97**, 124302 (2006).
[7] D. M. T. Kuo and Y. C. Chang, Phys. Rev. B **81**, 205321 (2010).
[8] Y. C. Tseng, D. M. T. Kuo, Y. C. Chang and Y. T. Lin, Appl. Phys. Letts. **103**, 053108 (2013).
[9] MJ. Martinez, A. Fornieri and F. Giazotto, Nature Nanotechnology, **10**, 303 (2015).
[10] J. P. Bergfield and C. A. Stafford, Nano Letters **9**, 3072 (2009).
[11] J. P. Bergfield, M. A. Solis, and C. A. Staffford, ACS Nano **4**, 5314 (2010).
[12] C. C. Chen, Y. C. Chang and David M T Kuo, Phys. Chem. Chem. Phys. **17**, 6606 (2015).
[13] C. C. Chen, David M T Kuo and Y. C. Chang, Phys. Chem. Chem. Phys. **17**, 19386 (2015).
[14] H. Haug and A. P. Jauho, Quantum Kinetics in Transport and Optics of Semiconductors (Springer, Heidelberg, 1996).
[15] A. P. Jauho, N. S. Wingreen and Y. Meir, Phys. Rev. B **50**, 5528 (1994), and references therein.
[16] David M. T. Kuo and Y. C. Chang, Nanotechnology, **24**, 175403 (2013).
[17] S. F. Svensson, E. A. Hoffmann, N. Nakpathomkun, P. M. Mu, H. Q. Xu, H. A. Nilsson, D. Sanchez, V. kashcheyevs and H. Linke, New. J. Phys. **15**, 105011 (2013).
[18] N. Nakpathomkun, H. Q. Xu and H. Linke, Phys. Rev. B **82**, 235428 (2010).
[19] M. Leijnse, M. R. Wegewijs and K. Flensberg, Phys. Rev. B **82**, 045412 (2010).
[20] Y. S. Liu, X. F. Yang, X. K. Hong, M. S. Si, F. Chi and Y. Guo. App. Phys. Lett, 103, 093901 (2013).
[21] H. Thierschmann, F. Arnold, M. Mittermuller, L. Maier, C. Heyn, W. Hansen, H. Buhmann and L. W Molenkamp, New. J. Phys. 17, 113003 (2015).
[22] David M. T. Kuo and Y. C. Chang, Phys Rev. B, **89**, 115416 (2014).
[23] D. M. T. Kuo, S. Y. Shiau and Y. C. Chang, Phys. Rev. B. **84**, 245303 (2011).
[24] J. Zhu, K. Hippalgaonkar, S. Shen, KV Wang, Y. Abate, S. Lee, J. Wu, X. Yin, A. Majumdar and X. Zhang, Nano Lett, 14, 4867 (2014).
[25] H. Thierschmann, R. Sanchez, B. Sothmann, F. Arnold, C. Heyn, W. Hansen, , H. Buhmann and L. W. Molenkamp, Nature Nanotechnolgy, 10, 854(2015).
[26] B. Sothmann, R. Sanchez and A. N. Jordan, Nanotechnolgy, 26, 032001(2015).

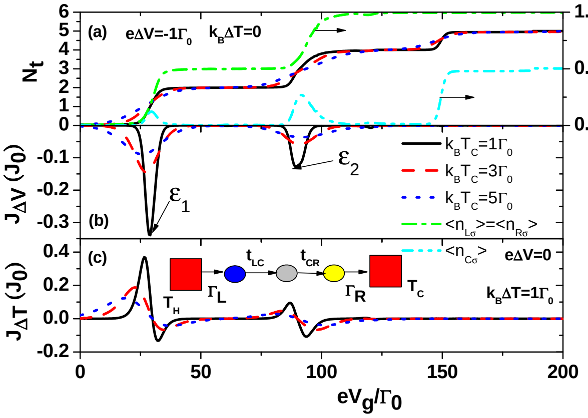

FIG. 1: (a) Total occupation number, (b) charge current ($J_{\Delta V}$) at $k_B\Delta V = -1\Gamma_0$ and $k_B\Delta T = 0$, and (c) charge current ($J_{\Delta T}$) at $e\Delta T = 1\Gamma_0$ and $k_B\Delta V = 0$ as a function of quantum dot energy levels ($E_\ell = E_0 = E_F + 30\Gamma_0 - eV_g$) for different T_C temperatures. We have following physical parameters $t_{LC} = t_{CR} = 1\Gamma_0$, $t_{LR} = 0$, $U_\ell = 60\Gamma_0$, $U_{LC} = U_{CR} = 30\Gamma_0$, and $\Gamma_L = \Gamma_R = \Gamma = 1\Gamma_0$. $J_0 = e\Gamma_0/h$

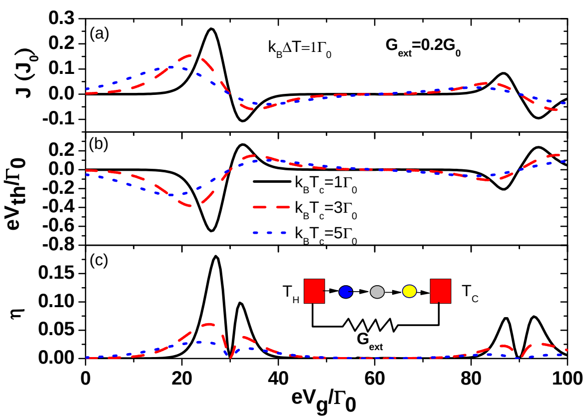

FIG. 2: (a)Charge current (J), (b) thermal voltage (eV_{th}) and (c) efficiency (η) as a function of QD energy level ($E_\ell = E_F + 30\Gamma_0 - eV_g$) for different T_C values at $k_B\Delta T = 1\Gamma_0$. Other physical parameters are the same as those of Fig. 1. Other physical parameters are the same as those of Fig.1. $G_{ext} = 0.2G_0$, where $G_0 = 2e_0^2/h$.

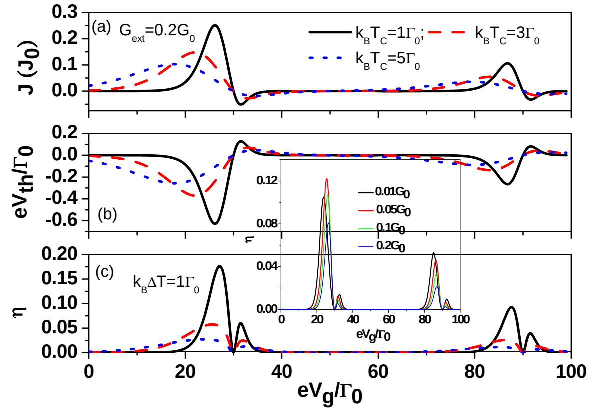

FIG. 3: (a)Charge current (J), (b) thermal voltage (eV_{th}) and (c) efficiency (η) as a function of QD energy level ($E_\ell = E_F + 30\Gamma_0 - eV_g$) for different T_C values at $k_B\Delta T = 1\Gamma_0$. The curves of Fig. 3 are one to one corresponding to those of Fig.2. The inset of Fig. 3 shows the η for four G_{ext} values; $0.01, 0.05, 0.1$ and $0.2G_0$ at $k_BT_C = 1\Gamma_0$.

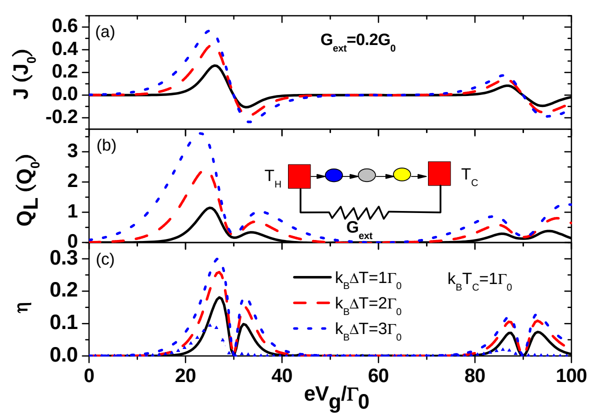

FIG. 4: (a) Charge current (J), (b) heat current (Q_L) and (c) efficiency η as a function of QD energy level for different $k_B\Delta T$ values at $T_C = 1\Gamma_0$. We have heat flow in units of $Q_0 = \Gamma_0^2/h$. Other physical parameters are the same as those of Fig. 1.

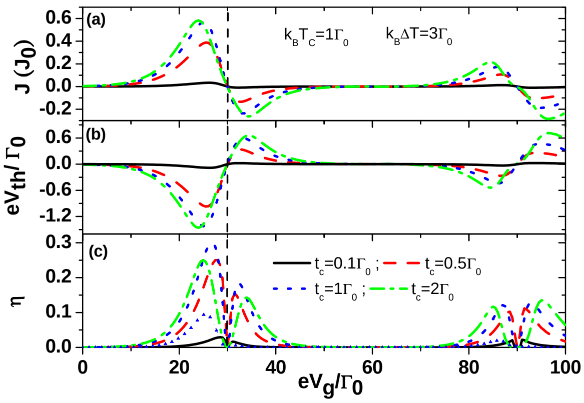

FIG. 5: (a) Charge current, (b) heat current (Q_L) and (c) efficiency (η) as a function of QD energy levels for different t_c values at $k_B\Delta T = 3\Gamma_0$, and $k_BT_C = 1\Gamma_0$. Other physical parameters are the same as those of Fig. 1.The curve with triangle marks is duplicated from Fig. 4(c) to reveal the Q_{ph} effect.

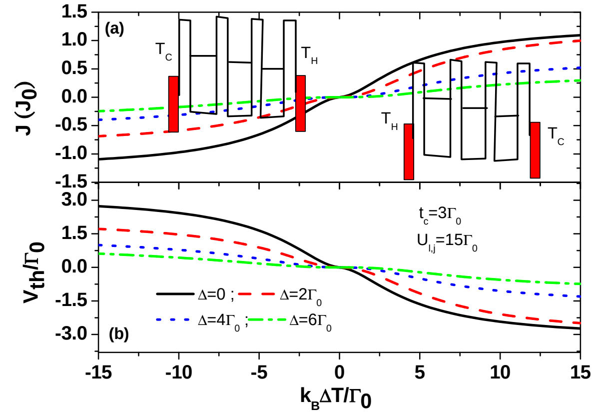

FIG. 7: (a) Charge current (J) and (b) thermal voltage (V_{th}) as functions of temperature bias for different QDM configurations ($E_R = E_F + 10\Gamma_0$, $E_C = E_R + \Delta$, and $E_L = E_R + 2\Delta$) with $t_c = 3\Gamma_0$, $U_{\ell,j} = 15\Gamma_0$, and $T_c = 1\Gamma_0$. We have considered QD energy levels shifted by the V_{th}. Here $E_{L(R)}$ is replaced by $\epsilon_{L(R)} = E_{L(R)} \pm 0.3V_{th}$. Other physical parameters are the same as those of Fig. 1.

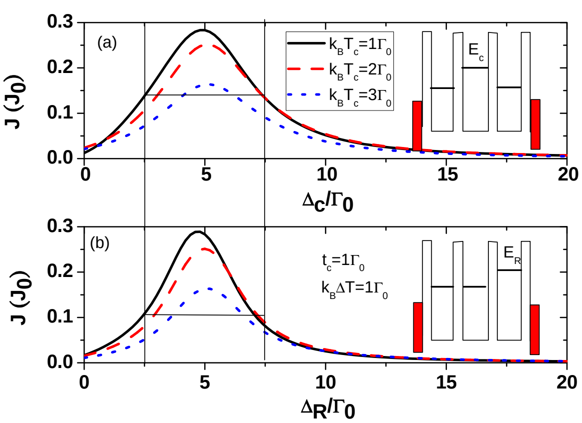

FIG. 6: Charge current (J) as a function of QD energy levels for different T_C values at $t_c = 1\Gamma_0$ and $k_B\Delta T = 1\Gamma_0$. (a) $E_L = E_R = E_F + 5\Gamma_0$ and the energy level of center QD (E_c) is varied ($\Delta_C = E_C - E_F$).(b) $E_L = E_C = E_F + 5\Gamma_0$ and the energy level of one outer QD (E_R) is varied ($\Delta_R = E_R - E_F$). Other physical parameters are the same as those of Fig. 4.

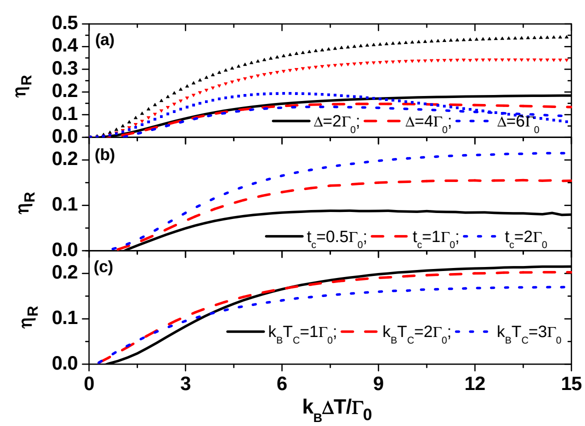

FIG. 8: Charge current rectification efficiency (η_R) as a function of temperature bias for the variations of different physical parameters; (a) Δ values at $t_c = 3\Gamma_0$, and $T_c = 1\Gamma_0$, (b) t_c values at $\Delta = 2\Gamma_0$ and $T_c = 1\Gamma_0$, and (c) T_c values at $\Delta = 2\Gamma_0$ and $t_c = 2\Gamma_0$. Other physical parameters are the same as those of Fig. 7.